Title: Delivery of self-amplifying mRNA vaccines by cationic lipid nanoparticles: The impact of cationic lipid selection

Authors: Gustavo Lou[1,2], Giulia Anderluzzi[1,2], Signe Tandrup Schmidt[1,4], Stuart Woods[1], Simona Gallorini[2], Michela Brazzoli[2], Fabiola Giusti[2], Ilaria Ferlenghi[2], Russell Johnson[3], Craig W. Roberts[1], Derek T. O'Hagan[3], Barbara C. Baudner[2]* and Yvonne Perrie[1]*

[1]Strathclyde Institute of Pharmacy and Biomedical Sciences, University of Strathclyde, 161 Cathedral St., G4 0RE Glasgow, Scotland.

[2]GSK, Siena, Italy.

[3]GSK, Rockville, United States

[4]Department of Infectious Disease Immunology, Center for Vaccine Research, Statens Serum Institut, Artillerivej 5, 2300 Copenhagen S, Denmark

Key Words: Self-amplifying RNA, lipid nanoparticles, microfluidics, cellular uptake, in vitro potency, pharmacokinetics, immunogenicity

Corresponding author:

Professor Yvonne Perrie

Strathclyde Institute of Pharmacy and Biomedical Sciences,

161 Cathedral St,

University of Strathclyde,

Glasgow, G4 0RE

Scotland.

yvonne.perrie@strath.ac.uk

Abstract

Self-amplifying RNA (SAM) represents a versatile tool that can be used to develop potent vaccines, potentially able to elicit strong antigen-specific humoral and cellular-mediated immune responses to virtually any infectious disease. To protect the SAM from degradation and achieve efficient delivery, lipid nanoparticles (LNPs), particularly those based on ionizable amino-lipids, are commonly adopted. Herein, we compared commonly available cationic lipids, which have been broadly used in clinical investigations, as an alternative to ionizable lipids. To this end, a SAM vaccine encoding the rabies virus glycoprotein (RVG) was used. The cationic lipids investigated including 3ß-[N-(N',N'-dimethylaminoethane)-carbamoyl]cholesterol (DC-Chol), dimethyldioctadecylammonium (DDA), 1,2-dioleoyl-3-trimethylammonium-propane (DOTAP), 1,2-dimyristoyl-3-trimethylammonium-propane (DMTAP), 1,2-stearoyl-3-trimethylammonium-propane (DSTAP) and N-(4-carboxybenzyl)-N,N-dimethyl-2,3-bis(oleoyloxy)propan-1-aminium (DOBAQ). Whilst all cationic LNP (cLNP) formulations promoting high association with cells in vitro, those formulations containing the fusogenic lipid 1,2-dioleoyl-sn-3-phosphoethanolamine (DOPE) in combination with DOTAP or DDA were the most efficient at inducing antigen expression. Therefore, DOTAP and DDA formulations were selected for further in vivo studies and were compared to benchmark ionizable LNPs (iLNPs). Biodistribution studies revealed that DDA-cLNPs remained longer at the injection site compared with DOTAP-cLNPs and iLNPs when administered intramuscularly in mice. However, both the cLNP formulations and the iLNPs induced strong humoral and cellular-mediated immune responses in mice that were not significantly different at a 1.5 µg SAM dose. In summary, cLNPs based on DOTAP and DDA are an efficient alternative to iLNPs to deliver SAM vaccines.

Introduction

The ability of nucleic acids (pDNA and mRNA) to induce antigen expression in vivo was first reported three decades ago by Wolff et al. [1]. Subsequent investigations demonstrated that antigens expressed by delivered nucleic acids were able to induce immune responses to the encoded antigens. These findings led to remarkable interest in the field of nucleic acid-based vaccines [2]. As with viral vector and DNA-based vaccines, mRNA vaccines can induce humoral and type-1 cellular-mediated immune responses; moreover, they do not require nucleus importation and genome integration. mRNA vaccines also have the potential to be produced in an inexpensive and scalable manner by means of synthetic manufacturing processes. This makes mRNA vaccines a unique platform to fight newly emerging diseases [3]. mRNA vaccines can be engineered in the form of self-amplifying mRNA

(SAM) based on an alphavirus genome, where the genes encoding the structural proteins are substituted by the antigen gene of interest. Due to their self-amplifying properties, SAM vaccines induce prolonged local antigen expression [4], and are able to elicit robust immune responses with significantly lower doses as compared to conventional mRNA vaccines [5].

The highly anionic and hydrophilic nature of mRNA impairs its cellular uptake. After being taken up by host cells, mRNA is degraded in the endo-lysosomal compartments. Furthermore, extracellular RNases quickly degrade mRNA molecules thus limiting their potency, so that high doses of naked mRNA are needed to elicit immune responses [6]. These barriers can be overcome using delivery systems such as cationic nanoemulsions (CNE) [7], polyplexes [8] and, in particular, lipid nanoparticles (LNPs) [9]. Among LNPs, those containing ionizable amino-lipids with pKa values of 6-7 are the most efficient [10]. An ionizable LNP (iLNP) formulation based on the ionizable lipid DLin-MC3-DMA (pKa = 6.44) was approved by the FDA in 2018. This iLNP formulation, enclosing a therapeutic siRNA (patisiran) for the treatment of hereditary transthyretin mediated amyloidosis, became the first siRNA-based product to be licenced (trade name Onpattro). Although iLNPs were optimized to deliver small interfering RNA (siRNA) intravenously, they they are efficient delivery systems for mRNA [11] and SAM vaccines [12]. This has resulted in a number of iLNP-formulated mRNA and SAM vaccines being investigated in clinical trials for the treatment of various infectious diseases, including chikungunya, influenza, zika virus, rabies virus and human cytomegalovirus [3].

Optimal mRNA and siRNA-LNP formulation properties have been shown to differ. The pKa of the ionizable lipid is a strong determinant in the potency of siRNA-LNP systems. Systematic studies conducted with broad lipid libraries reported that the maximum activity of siRNA-iLNP systems is achieved with a pKa value around 6.4 [10]. In contrast, it was recently suggested that the ideal pKa value of mRNA-iLNP formulations was 6.6-6.8, although other factors (e.g. LNP size) played a role on their immunogenicity [13] and Kauffmann et al. [14] highlighted the differences between mRNA and siRNA delivery by using Design of Experiments (DOE). An iLNP formulation based on the lipid C12-200, previously used to deliver siRNA, was optimized to deliver a mRNA encoding erythropoietin intravenously. The incorporation of DOPE within the formulation and higher C12-200:mRNA ratios increased the potency of mRNA-LNPs 7-fold, while no improvement was observed for siRNA-LNPs. These findings further supported that the in vivo efficacy of mRNA LNPs is governed by other factors apart from the pKa of the ionizable lipid.

Despite ionizable lipids have recognised ability to deliver mRNA, they may be, in some cases, considerably more expensive than existing cationic lipids (e.g. DOTAP). Furthermore, from a regulatory and safety perspective, there is less clinical data available on the use of novel ionizable lipids. In

contrast, cationic lipids have been extensively investigated to deliver subunit antigens [15], DNA [16] and non-amplifying mRNA [17] and have demonstrated an acceptable safety profile. Hence, formulations based on well-established lipids could facilitate and accelerate the pharmaceutical development of mRNA and SAM vaccines. Herein, we tested a panel of cationic LNPs (cLNPs), based on conventional cationic lipids to deliver a SAM vaccine and compared them along with benchmark iLNPs described by Geall et al. [4]. To this end, the rabies virus was selected as a model to evaluate delivery vehicles for SAM, owing the availability of an efficacious commercial vaccines (e.g. Rabipur) and an established correlate of protection (neutralizing antibodies). Because the rabies virus glycoprotein (RVG) is the only target for neutralizing antibodies and the only antigen to confer protection against challenge [18], a SAM vaccine encoding RVG (RVG-SAM) was used. We selected most promising formulations according to their physicochemical attributes (size, size distribution and SAM encapsulation efficiency), their cellular uptake and in vitro potency. These formulations were investigated in vivo and compared to benchmark iLNPs. We hypothesized that these formulations could be efficient delivery systems for SAM.

Materials and Methods

Materials

1,2-distearoyl-sn-glycero-3-phosphocholine (DSPC), 1,2-dioleoyl-sn-3-phosphoethanolamine (DOPE), 3ß-[N-(N',N'-dimethylaminoethane)-carbamoyl]cholesterol (DC-Chol), dimethyldioctadecylammonium (DDA), 1,2-dioleoyl-3-trimethylammonium-propane (DOTAP), 1,2-dimyristoyl-3-trimethylammonium-propane (DMTAP), 1,2-stearoyl-3-trimethylammonium-propane (DSTAP), N-(4-carboxybenzyl)-N,N-dimethyl-2,3-bis(oleoyloxy)propan-1-aminium (DOBAQ) and 1,2-dimyristoyl-sn-glycero-3-phosphoethanolamine-N-[methoxy(polyethylene glycol)-2000] (DMG-PEG2000) were obtained from Avanti Polar Lipids. Penicillin-streptomycin, L-glutamine, cholesterol (Chol) and brefeldin A (BFA) were purchased from Sigma. RNase A, proteinase K, Northern Max formaldehyde load dye, Northern Max running 10X buffer, Ambion millennium RNA, SYBR gold nucleic acid stain marker (10,000X in DMSO), 3 M sodium acetate buffer pH 5.2, Ribo Green RNA assay kit, 1,1'-dioctadecyl-3,3,3',3'-tetramethylindocarbocyanine perchlorate (Dil-C_{18}), 1,1'-Dioctadecyl-3,3,3',3'-Tetramethylindotricarbocyanine Iodide (DiR), Lipofectamine2000, Opti-MEM, Alexa Fluor 488-labeled goat anti-mouse IgG2a Cross-Adsorbed secondary antibody and allophycocyanin (APC) Zenon antibody labelling kit for mouse IgG2a were purchased from Thermo Fisher. Dulbecco's Modified Eagle Medium (DMEM), Roswell Park Memorial Institute 1640 medium (RPMI-1640), Hank's balance salt solution (HBSS) trypsin-EDTA (0.25%) and foetal bovine serum (FBS) were obtained from

Gibco. Mini Ready Agarose precast gels 1% TAE and PLATELIA Rabies II Kit were obtained from Bio-Rad. 100 mM citrate buffer pH 6.0 was purchased from Teknova. Live/dead fixable dead cell stain near-IR was purchased from Life Technologies. Mouse anti-rabies glycoprotein antibody (clone 24-3F-10) was obtained from Merck. 10X Perm/Wash buffer and Cytofix/Cytoperm were obtained from BD Biosciences. Anti-mouse PE-CF594-conjugated CD8, V421-conjugated CD44, PE-conjugated TNF-α and BV786-conjugated IFN-γ monoclonal antibodies and anti-mouse Ig, κ/negative control compensation particles set were obtained from BD Bioscience. Anti-mouse BV510-conjugated CD4, APC-conjugated CD3 and PE-Cy5-conjugated IL-2 monoclonal antibodies and RBC lysis buffer were purchased from Biolegend. Anti-mouse PE-Cy7-conjugated IL-17, CD28 and CD3 monoclonal antibodies was purchased from ePharmingen. The rabies peptide pool containing peptides of 15-mers with 11 amino acid overlap were obtained from Genescript.

Synthesis of self-amplifying RNA (SAM)

A self-amplifying RNA (SAM) vaccine encoding the rabies virus glycoprotein (RVG) was synthesized as previously described [4]. In brief, DNA plasmids encoding the RVG-SAM were constructed using standard molecular techniques. Plasmids were amplified in *Escherichia coli* and purified using Qiagen Plasmid Maxi kits (Qiagen). DNA was linearized following the 3' end of SAM sequence by restriction digest. Linearized DNA templates were transcribed into RNA using a MEGAscript T7 kit (Life Technologies) and purified by LiCl precipitation. RNA was then capped using the Vaccinia Capping system (New England BioLabs) and purified by LiCl precipitation before formulation.

Formulation of SAM lipid nanoparticles (SAM-LNPs)

SAM-cLNPs were produced in the NanoAssemblr Platform (Precision NanoSystems Inc., Vancouver) in a Y-shaped staggered herringbone micromixer of 300 µm width and 130 µm height. LNPs were composed of 1) DOPE, a cationic lipid and DMG-PEG2000 at 49:49:2 molar ratio or 2) or DSPC, Chol, a cationic lipid and DMG-PEG2000 at 10:48:40:2 molar ratio. Lipids dissolved in methanol an aqueous phase containing SAM were injected simultaneously in the micromixer. SAM-cLNPs were produced at 4-8 mg/mL lipid concentration, 3:1 aqueous:organic flow rate ratio (FRR), 5 mL/min total flow rate (TFR). SAM was injected in 100 mM citrate buffer pH 6.0 with an 8:1 N:P mole ratio (N in the cationic lipid and P in SAM). Benchmark iLNPs described by Geall et al [4] were produced in the same manner. Newly formed SAM-cLNPs and iLNPs (1 mL) were dialyzed against 10 mM TRIS pH 7.4 (200 mL) for 1 hour under magnetic stirring. For in vivo studies, SAM-cLNPs were dialyzed against 100 mM TRIS buffer pH 7.4.

Formulation of cationic nanoemulsion (CNE)

As a comparator, DOTAP-based CNE (DOTAP-CNE) was prepared as previously described [7]. A mixture of squalene, DOTAP, sorbitan trioleate and polysorbate 80 (4.3, 0.4, 0.5 and 0.5% w/w) was homogenized for 2 minutes in a T25 homogenizer (IKA) at 24 KRPM to produce a primary emulsion and then passes through a M-110P Microfluidizer (Microfluidics) at a pressure of 20,000 PSI. RVG-SAM (300 µg/mL) and DOTAP-CNE were mixed in equals volumes and allowed to complex on ice for 30 minutes. Prior to administration, DOTAP-CNE was diluted to dosing concentration.

Physicochemical characterization

SAM-LNPs were characterized in terms of hydrodynamic size (Z-average), polydispersity index (PDI) and surface charge (zeta-potential) by dynamic light scattering (DLS) in a Zetasizer Nano ZS (Malvern, UK) at 0.1 mg/mL at 25 ˚C. The SAM encapsulation/adsorption efficiency (SAM E.E.) was quantified by Ribo Green assay following manufacturer instructions. Fluorescence was measured at excitation and emission wavelength of 485 and 528 nm in a Synergy H1 microplate Reader (BioTek). SAM E.E. was calculated as as $(F_T - F_0)/F_T$ were F_T and F_0 are the amount of SAM quantified in presence and absence of 1 % triton X-100.

Cellular association and transfection efficiency

A total of 50,000 BHK cells were cultured per well in 24-well plates in RPMI in presence (5%) or absence of heat-inactivated foetal bovine serum (HI-FBS) and allowed to adhere for 8 hours at 37 °C and 5% CO_2. Cells were then incubated with RVG-SAM LNPs in presence (5%) or absence of HI-FBS. As a control, cells were treated with Lipofectamine2000-transfected SAM following manufacturer instructions. After 16 hours, cells were fixed and permeabilized with Cytofix/Cytoperm (100 µL/well) and incubated with a mouse anti-RVG monoclonal antibody (1:1000) for 1 hour at room temperature and then with an Alexa Fluor 488-labelled goat anti-mouse IgG2a antibody (1:1000) for 1 hour at room temperature. The percentage of transfected BHK cells was then analyzed by flow cytometry (FACSCanto, BD Biosciences) with respect to untreated cells. For cellular uptake experiments, LNPs were co-formulated with the lipophilic fluorescent dye Dil-C_{18} (0.2% mole %) as previously described [19].

RNase protection assay

A total of 2.8 µg SAM (200 µL), either naked or encapsulated in cLNPs were challenged with 0.028 µg RNase A (20 µL) for 30 min at room temperature, followed by an incubation with 0.14 µg of recombinant proteinase K for 10 min at 55 °C. Subsequently, 750 µL of ethanol and 25 µL of 3 M sodium acetate pH 5.2 were added to each sample, which were then centrifuged at 14,000 rpm for 20 min. Ethanol precipitation and centrifugation was repeated twice. SAM pellets were resuspended in

35 µL of DEPC-treated water, mixed with formaldehyde load dye (1:3 v/v) and heated at 65 °C for 10 min and then cooled to room temperature. The equivalent of 200 ng of SAM (10 µL) were loaded in a denatured 1% agarose gel in Northern Max 3-(N-morpholino)propane sulfonic acid (MOPS) running buffer, containing 0.1 % of SYBR gold stain, and run at 90 V. Ambion Millennium marker was used as the molecular weight standard. Gel images were acquired in a Gel Doc EZ imager (Bio-Rad).

Cryo-TEM

Aliquots of 2.3 µL of each sample were applied onto glow-discharged Quantifoil R2/2 grids and vitrified by using a Vitrobot (FEI Company, Eindhoven, The Netherlands). The vitrified grids were mounted on a pre-equilibrated cryo-holder and subsequently inserted into a cryo-TEM (FEG 200-FEI) microscope operating at 200kV and observed under low-electron dose conditions. All samples were imaged with a TVIPS TemCam F224HD CCD camera at 50,000X magnification with pixel size 0.33 nM.

Immunization studies

All animal studies were ethically reviewed and carried out in accordance with European Directive 2010/63/EEC and the GSK policy on the Care, Welfare and Treatment of Animals. Groups of ten 7-weeks-old female BALB/c mice (Charles River) were immunized intramuscularly on days 0 and 28 in their right and left thighs (25 µL per site) with RVG-SAM (1.5 or 0.15 µg/dose) formulated in either DOTAP-cLNPs, DDA-cLNPs or benchmark iLNPs [4]. Two further groups of mice were vaccinated with the same doses of RVG-SAM formulated in DOTAP-CNE, a safe and well-established SAM delivery system [7] currently being investigated in a phase I clinical trial in humans (NCT04062669). A group of mice was immunized with 50 µL of the commercial vaccine Rabipur (trademark owned by GSK group of companies), corresponding to 5% of the human dose (HD). Sera from individual mice were collected four weeks after first vaccination (day 28) and two weeks after second vaccination (day 42) and pooled in pools of two sera each. Spleens from 3 randomly selected mice from each group were collected two weeks after the second immunization to perform a T cell assay *in vitro*.

Immunological readouts

Total anti-RVG IgG titers were quantified with the PLATELIA RABIES II Kit *Ad Usum Veterinarium* [20] following manufacturer instructions. T cell responses were quantified as follows. Spleens from 3 randomly selected mice from each experimental group were taken on day 42 (two weeks after second vaccination). Single cell suspensions were obtained as previously described [21]. Spleens were pushed, in cold HBSS, through 70 µm cell strainers and washed with HBSS. Samples were then incubated with RBC lysis buffer (2 mL) at 4 °C for 2 minutes. Subsequently, they were resuspended in complete RPMI (cRPMI) and passed again through cell strainers. Cells were counted in a Vi-CELL XR cell counter

(Beckman Coulter). A total of $1.5 \cdot 10^6$ splenocytes were cultured per well in round-bottomed 96-well plates. Splenocytes were stimulated with a RVG-derived peptide pool library (2.5 μg/mL) consisting on 15-mers with 11 amino acid overlaps andanti-CD28 (2 μg/mL) in presence of brefeldin A (5 μg/mL) for 4 hours at 37 °C. Cells were also stimulated with anti-CD3 (1 μg/mL) plus anti-CD28 (2 μg/mL) or anti-CD28 alone as positive and negative controls respectively. Samples were then stained with a live/dead fixable near-IR dead cell stain kit, then fixed and permeabilized with Cytofix/Cytoperm and subsequently stained with the following antibodies in Perm/Wash Buffer: APC-conjugated anti-CD3, BV510-conjugated anti-CD4, PE-CF594-conjugated anti-CD8, BV785-conjugated anti-IFN-γ, PE-Cy5-conjugated anti-IL-2, anti-BV605-conjugated TNF-α and PE-Cy7-conjugated anti-IL-17. Samples were acquired in a LSR II flow cytometer (BD Biosciences) and analyzed in FlowJo Software (Tree Star). Antigen-specific $CD4^+$ T cell subsets were identified based on the combination of secreted cytokines as follows: Th1 (IFN-γ^+ IL-2^+ TNF-α^+; IFN-γ^+ IL-2^+; IFN-γ^+ TNF-α^+; IFN-γ^+); Th0 (IL-2^+ TNF-α^+; IL-2^+; TNF-α^+). The frequency of antigen-specific $CD8^+$ T cells were identified based on the combination of IFN-γ^+, IL-2^+ and TNF-α^+.

Biodistribution studies

Biodistribution studies were ethically reviewed and carried out in accordance with European Directive 2010/63/EEC. All protocols were carried out in a designated establishment in the animal facility at the University of Strathclyde (Glasgow, UK) conforming to the guidelines from the Home Office of the UK government under the Animals [Scientific Procedures] Act 1986. All work was carried out under a project license with approval from the University of Strathclyde Ethical Review Board. In order to track their biodistribution in vivo, cLNPs and iLNPs were co-formulated with the lipophilic fluorescent dye 1,1'-Dioctadecyl-3,3,3',3'-Tetramethylindotricarbocyanine Iodide (DiR) as previously described [22]. Groups of five 6-8-week-old female balb/c mice were housed in polypropylene cages (13cm×35cm), containing Ecopure flakes and sizzle nest bedding (SDS Services) with access to water and CRM mouse chow (SDS Services) *ad libatim*. Groups were assigned at random by technical staff with no knowledge of the experimental purpose and the minimum number of mice were used to give statistical significance. Mice Imaging was carried out using an IVIS Spectrum (Perkin Elmer) using Living Image software for data capture and analysis. The presence of DiR was detected using an excitation wavelength of 710nm and an emission filter of 780nm. A medium binning and f/stop of 2 was used and acquisition time was determined for each image with auto-exposure settings. Mice were anaesthetized for imaging using 3% Isoflurane. Anaesthesia was maintained during imaging at 1% Isoflurane. Images were taken before and after administration of formulations after 4, 24, 48, 72, 144

and 240 hours post injection. The total flux (p/s) was calculated at the injection site (region of interest) for each mouse.

Statistical Analysis

Statistical analysis of cellular uptake, in vitro potency, T cell responses and biodistribution experiments was performed by one-way analysis of variance (ANOVA) followed Tukey's honest significance test. Statistical analysis of IgG titers was performed by Kruskal-Wallis followed by Dunn's test. P values below 0.05 (*) were considered significant. All analyses were done in GraphPad Prism 7.0.

Results

Physicochemical characterization of SAM-cLNPs

A panel of cLNPs composed of the fusogenic lipid DOPE, a cationic lipid (DOTAP, DDA, DC-Chol, DMTAP, DSTAP or DOBAQ) and a DMG-PEG2000 (49:49:2 molar ratio) was produced in a microfluidic mixer (NanoAssemblr, Precision Nanosystems Inc.). Some cLNPs were prepared with a lipid composition of DSPC, Chol, a cationic lipid and DMG-PEG2000 (10:48:40:2 molar ratio) for a direct comparison with the lipid composition of benchmark iLNPs [23]. Benchmark iLNPs and those cLNPs based on DOTAP, DDA, DC-Chol, DMTAP and DOBAQ had an average hydrodynamic size ranging from 66 to 102 nm and a low PDI (<0.25), a neutral zeta-potential (<5 mV) and high SAM encapsulation efficiencies (SAM E.E.>85). In contrast, DSTAP-cLNPs had larger sizes (>300 nm), high PDI (>0.4) and lower SAM E.E. (<75%, Table 1). Therefore, DSTAP-cLNPs were not considered for further investigations. No significant differences were observed between DOPE-cLNPs and DSPC/Chol-C14-cLNPs.

Table 1. Physicochemical characterization of SAM-LNPs produced by microfluidics. Formulations were composed of DOPE, a cationic lipid and DMG-PEG2000 at 49:49:2 molar ratio or DSPC, Chol, a cationic lipid/ionizable lipid and DMG-PEG2000 at 10:48:40:2 molar ratio. E.E. (encapsulation efficiency); ZP (zeta-potential). Results are represented as mean ± of three independent experiments.

Cationic lipid	Composition (molar ratio)	Size (d.nm)	PDI	ZP (mV)	SAM E.E. (%)
DOTAP	49:49:2	83 ± 6	0.17 ± 0.05	3.1 ± 0.6	97 ± 2
	10:48:40:2	92 ± 5	0.23 ± 0.02	2.7 ± 0.4	99 ± 2
DDA	49:49:2	81 ± 9	0.13 ± 0.02	2.9 ± 0.7	98 ± 2
	10:48:40:2	80 ± 1	0.17 ± 0.02	2.4 ± 0.4	99 ± 1
DC-Chol	49:49:2	88 ± 6	0.16 ± 0.04	2.2 ± 1.9	91 ± 6
	10:48:40:2	88 ± 6	0.17 ± 0.03	1.3 ± 0.7	96 ± 4

DMTAP	49:49:2	86 ± 9	0.16 ± 0.02	2.2 ± 1.5	96 ± 3
	10:48:40:2	72 ± 2	0.15 ± 0.05	1.8 ± 0.6	98 ± 3
DSTAP	49:49:2	331 ± 70	0.89 ± 0.13	3.2 ± 0.3	70 ± 3
	10:48:40:2	472 ± 117	0.45 ± 0.10	3 ± 0.7	74 ± 4
DOBAQ	49:49:2	77 ± 2	0.22 ± 0.04	2.7 ± 1.0	85 ± 3
	10:48:40:2	66 ± 2	0.24 ± 0.02	1.9 ± 0.9	85 ± 2
Ionizable lipid	10:48:40:2	102 ± 4	0.10 ± 0.04	1.5 ± 1.3	98 ± 1

Cellular association and transfection efficiency of SAM-LNPs

The ability of SAM-LNPs to associate with cells and to induce antigen expression was investigated in vitro in baby hamster kidney cells (BHK). In the range of SAM concentrations tested, no cytotoxicity was observed (data not shown). Over 95% of BHK cells were found in association with cLNPs irrespective of the choice of cationic and "helper" lipids (DOPE or DSPC/Chol) and the presence or absence of serum proteins. In contrast, the cellular association of iLNPs was significantly ($p<0.05$) reduced in serum-free medium (Fig. 1A vs 1C). When considering the mean fluorescence intensity values, both the benchmark iLNPs and DOBAQ-based cLNPs were significantly ($p<0.05$) lower compared to cLNPs based on other cationic lipids, among which no significant differences were observed irrespective of the presence or absence of serum (Fig 1B and D respectively).

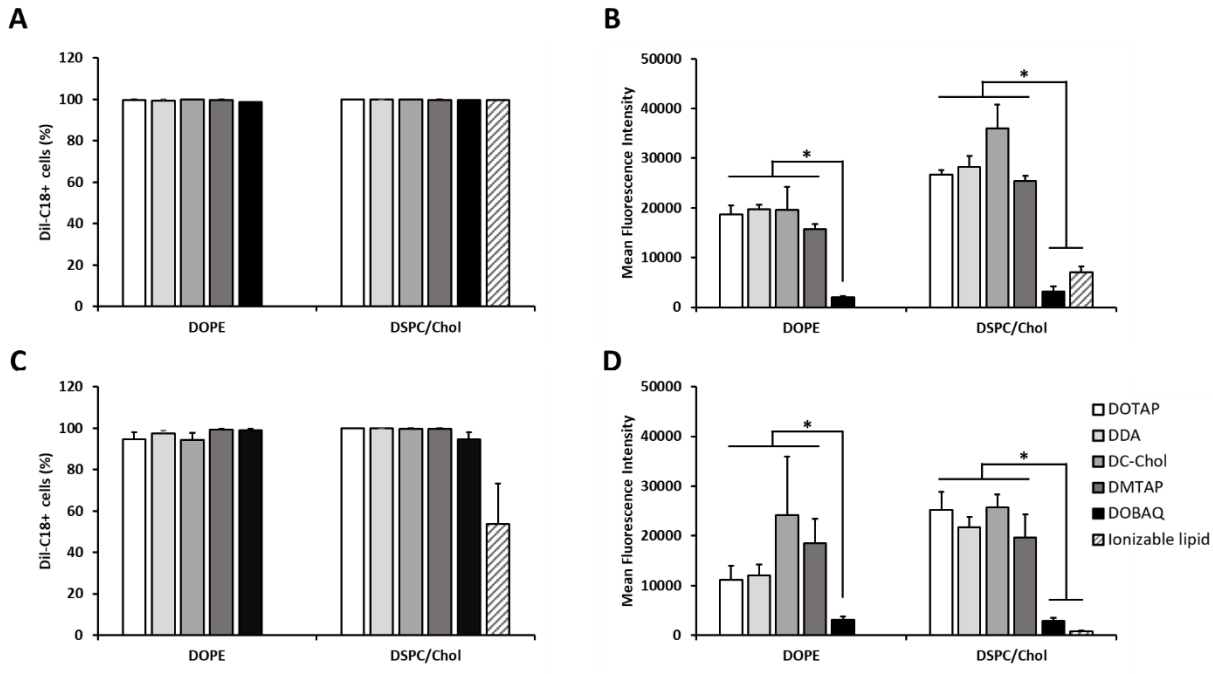

Figure 1. Cellular uptake RVG-SAM cLNPs and iLNPs in presence **(A, B)** and absence of 5% FBS **(C, D)** represented in terms of percentage of Dil-C_{18}^{+} cells **(A, C)** and mean fluorescence intensity **(B, D)**. cLNPs were composed of DOPE, a cationic (DOTAP, DDA, DC-Chol, DMTAP or DOBAQ) and DMG-PEG2000 at 49:49:2 mole % or DSPC, Chol, a cationic lipid and DMG-PEG2000 at 10:48:40:2 mole %. Results are represented as mean ± SD of three experiments. Statistical significance: $P < 0.05$ (*).

The next step was to investigate the in vitro potency of SAM-cLNPs (Fig. 2). When RVG-SAM was complexed with Lipofectamine2000, high frequencies of RVG^{+} cells were obtained irrespective of the presence or absence of FBS (Fig. 2). Ionizable LNPs promoted transfection of up to 35% of cells in presence of FBS (Fig. 2A) whereas they failed to induce RVG expression in FBS-free medium (Fig. 2B). When considering cLNPs, despite the high DSPC:Chol-cLNPs association with BHK cells shown in Fig. 1, these formulations induced low percentages of transfection even in absence of serum (<15% positive cells, data not shown). DOPE-based cLNPs prepared with either DOTAP or DDA were able to promote transfection in the presence of serum (Fig. 2A) and the potency of cLNPs was enhanced in serum-free medium, with the DOTAP and DDA formulations showing similar efficacy to LF2000 (approx. 90% RVG+ cells; Fig. 2B). Owing their improved in vitro potency, DOPE:DOTAP:DMG-PEG2000 and DOPE:DDA:DMG-PEG2000 cLNPs (named DOTAP and DDA-cLNPs henceforth) were the selected candidates for further studies.

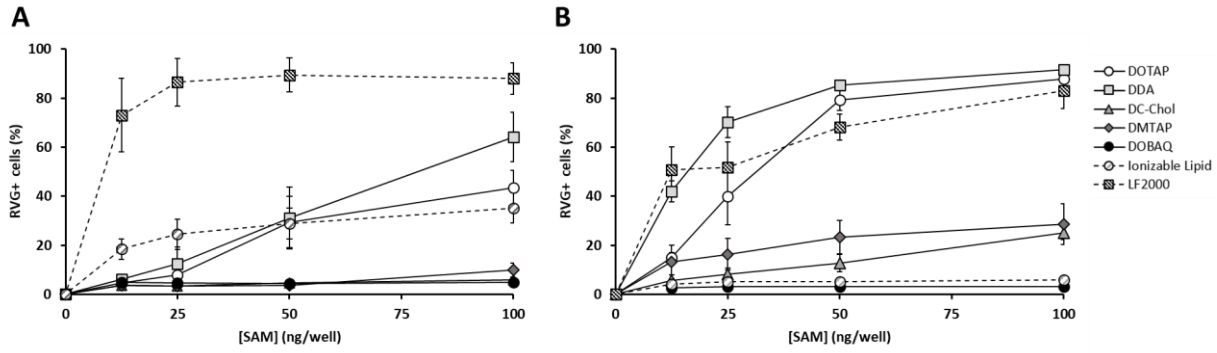

Figure 2. *In vitro* potency of RVG-SAM iLNPs and DOPE-cLNPs in presence **(A)** and absence of 5% FBS **(B)**. LF2000 (Lipofectamine2000). Results are represented as mean ± SD of three independent experiments.

The morphology of DOTAP and DDA-cLNPs was analyzed by cryo-electron transmission electron microscopy (Cryo-TEM). Both formulations formed spherical particles with diameters ranging from 40 to 80 nm (Fig. 3). They were heterogenous in terms of morphology of the particles, with some showing electron-dense cores and/or presence of a tightly packed bilayer. The DOTAP formulation had a prevalence of particles surrounded by a bilayer membrane with thickness around 5 nm, while DDA-

cLNPs had a bilayer of around 10 nm thickness. Furthermore, these cLNPs offered protection to RVG-SAM from degradation similar to iLNPs [4], whereas non-formulated RVG-SAM was completely degraded in presence of RNase A (Fig. S1).

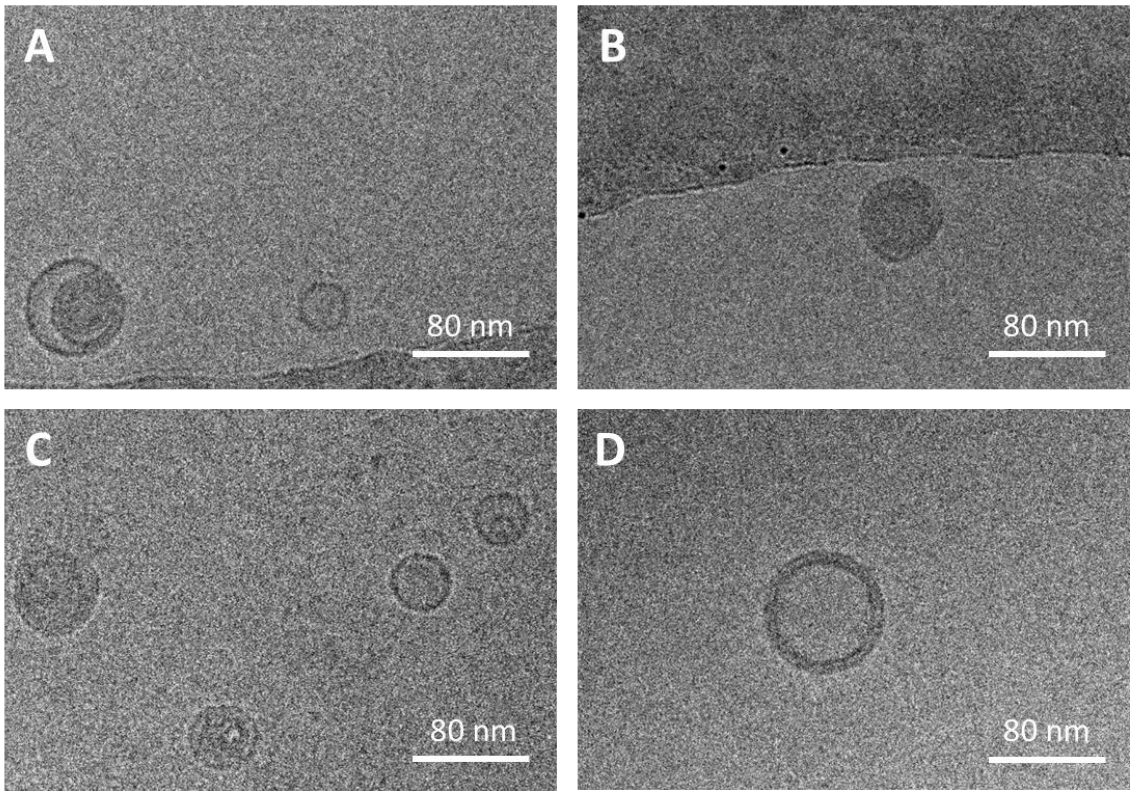

Figure 3. Cryo-TEM micrographs of DOTAP **(A, B)** and DDA-based SAM-cLNPs **(C, D)**.

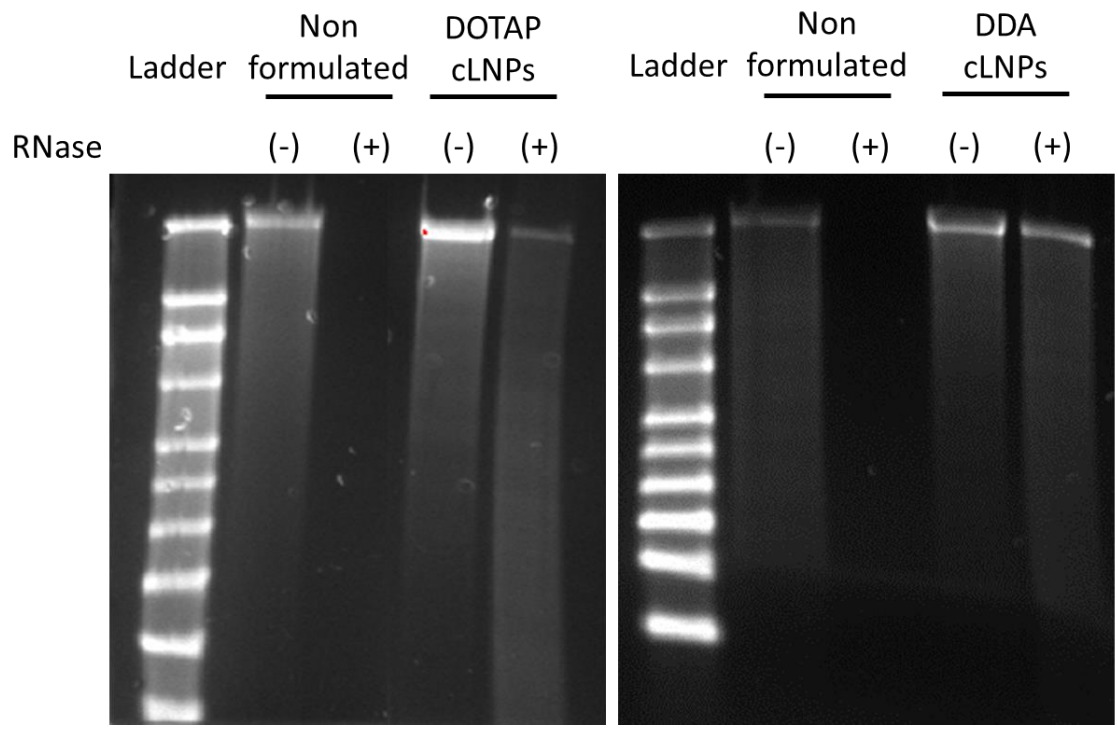

Figure S1. RNase A protection assay. RVG-SAM, either non-formulated or formulated in DOTAP or DDA-cLNPs, was challenged with RNase A and its integrity was analysed by agarose gel electrophoresis.

Immunogenicity of SAM-LNPs

Neutralizing antibodies (NAs) confer full protection against rabies infection and hence their production is critical [24]. We used the commercial PLATELIA Rabies II Kit (Bio-Rad), based on an enzyme-linked immunosorbent assay (ELISA) assay and by measuring total anti-RVG IgG titers (equivalent units/mL), the PLATELIA Rabies II Kit allows to indirectly quantify NAs [20].

Fig. 4A shows the results 27 days after the first immunisation using DOTAP and DDA cLNPs, DOTAP CNE and iLNPs, each at a RVG-SAM dose of 1.5 µg or 0.15 µg. After one immunisation with 1.5 µg SAM formulated in cLNPs, iLNPs or CNE, there were no significant differences among the antibody responses promoted and all responses were above the 0.5 EU/mL protection threshold. At the lower dose (0.15 µg), again there was no significant difference between the IgG titers promoted by the cLNPs and iLNPs and responses were above the protection threshold (Fig. 4A). Indeed, only the low dose of DOTAP-CNE giving significantly ($p<0.05$) lower responses compared to the iLNPs (Fig. 4A). These results show that when formulated in DOTAP or DDA-cLNPs, RVG-SAM at both the low and high dose elicited the production of anti-RVG IgGs above the correlate of protection two weeks after a single vaccination and that DOTAP and DDA-cLNPs were not significantly different in potency compared to iLNPs. SAM-cLNPs (1.5 µg) were also as potent as the commercial vaccine Rabipur. DOTAP-cLNPs and DOTAP-CNE induced similar immune responses were equally immunogenic when formulated with 1.5 µg RVG-SAM, but DOTAP-cLNPs seemed to induce a quicker onset of the immune response than DOTAP-CNE with a dose of 0.15 µg RVG-SAM (Fig. 4A). Two weeks after the second vaccination (Fig. 4B), total antibody titers increased up to 20-fold and clear dose-dependent immune responses were observed. After the second immunization with 1.5 µg SAM formulated in cLNPs, iLNPs or CNE, again there was no significant difference between the IgG immune responses promoted (Fig. 4B). At this dose, all formulations were as potent as the commercial vaccine Rabipur (Fig. 4B). However, at a lower dose (0.15 µg), the benchmark iLNPs were significantly ($p<0.05$) more immunogenic than cLNPs and CNE with geometric mean titers of 192, 10, 15 and 13 EU/mL for iLNPs, DOTAP-cLNPs, DDA-cLNPs and DOTAP-CNE respectively (Fig. 4B).

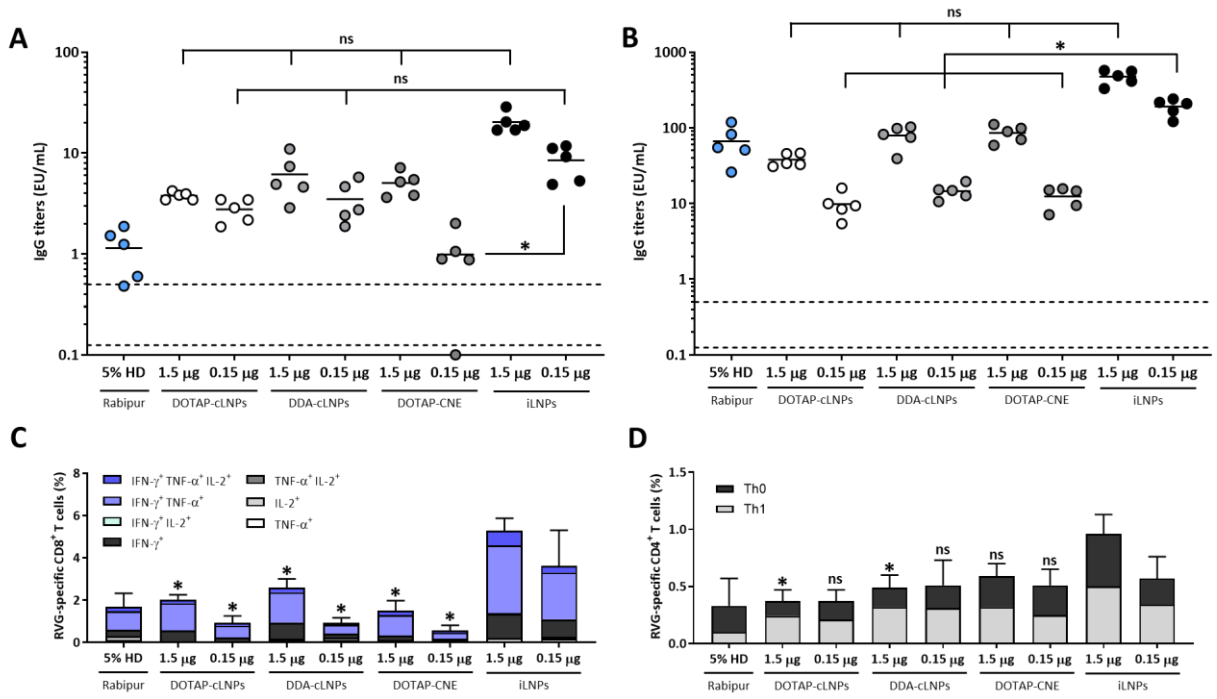

Figure 4. Total anti-RVG IgG titers in mice upon intramuscular injection of SAM formulated in cLNPs, DOTAP-CNE, iLNPs or the commercial vaccine Rabipur on days 0 and 28. Sera were collected after 27 **(A)** and 42 **(B)** days and total IgG titers were quantified using PLATELIA RABIES II KIT (Bio-Rad). Dots depict measurements from pools of 2 sera each. The solid lines represent the geometric mean titer (GMT) of each group (n=5). Dotted lines at 0.5 and 0.125 EU/mL correspond to protection threshold and limit of quantification respectively. *HD (human dose)*. **C)** Frequencies of RVG-specific cytokine producing $CD8^+$ **(C)** and $CD4^+$ T cells **(D)** analyzed with Boolean gates. $CD4^+$ T cells were represented as Th1 and Th0 cells according to secreted cytokines. T cell results are represented as mean ± SD of three replicates. For the statistical analysis of T cell responses, DOTAP-cLNPs, DDA-cLNPs and DOTAP-CNE were compared to iLNPs at the same SAM dose: non-significant (ns); $p < 0.05$ (*)

Cellular-mediated immunity plays a key role in virus clearance [25], and $CD4^+$ T cells are pivotal in mounting robust immune responses sustaining the production of NAs [26]. Hence, T cell responses were quantified after the second vaccination. Splenocytes from immunized mice were stimulated *in vitro* with an RVG-derived peptide pool and stained with a panel of antibodies to identify $CD4^+$ and $CD8^+$ T cells specific for selected cytokines (IFN-γ, TNF-α, IL-2 and IL-17). Finally, samples were analyzed by flow cytometry, following the gating strategy shown in Fig. S2 (as previously described [9]), to quantify and qualify RVG-specific T cells induced after vaccination. Most RVG-specific $CD8^+$ T cells had an effector Th1 phenotype, characterized by the production of IFN-γ alone or in combination with TNF-α and/or IL-2 (Fig. 4C). As can be seen, approximately 2% and 1% of cytokine producing $CD8^+$ T cells were quantified following vaccination with 1.5 and 0.15 µg RVG-SAM formulated in cLNPs and CNE, and a 1.5 µg RVG-SAM dose gave comparable responses to Rabipur (Fig. 4C). However, a significantly ($p<0.05$) higher frequency of $CD8^+$ T cells was quantified in the iLNP groups (5.3 and 3.6% for 1.5 and 0.15 µg RVG-SAM respectively; Fig. 4C). Similar to the IgG responses at the low RVG-SAM

dose, these frequencies were ranked in the order of iLNPs > DDA-cLNPs > DOTAP-cLNPs > DOTAP-CNE (Fig. 4C). $CD4^+$ T cells (Fig. 4D) were qualified based on the combination of expressed cytokines in Th1 (cells producing IFN- and its combinations) and Th0 (cells producing IL-2, TNF-α or a combination of both). No IL-17 producing T cells were detected. DOTAP and DDA-cLNPs induced similar frequencies of Th cells (0.5%) irrespective of the RVG-SAM dose, and these frequencies were comparable to DOTAP-CNE (Fig. 4D). However, at a 1.5 µg RVG-SAM dose, iLNPs induced significantly ($p<0.05$) higher frequencies of RVG-specific $CD4^+$ T cells compared to cLNPs but similar than CNE (Fig. 4D).

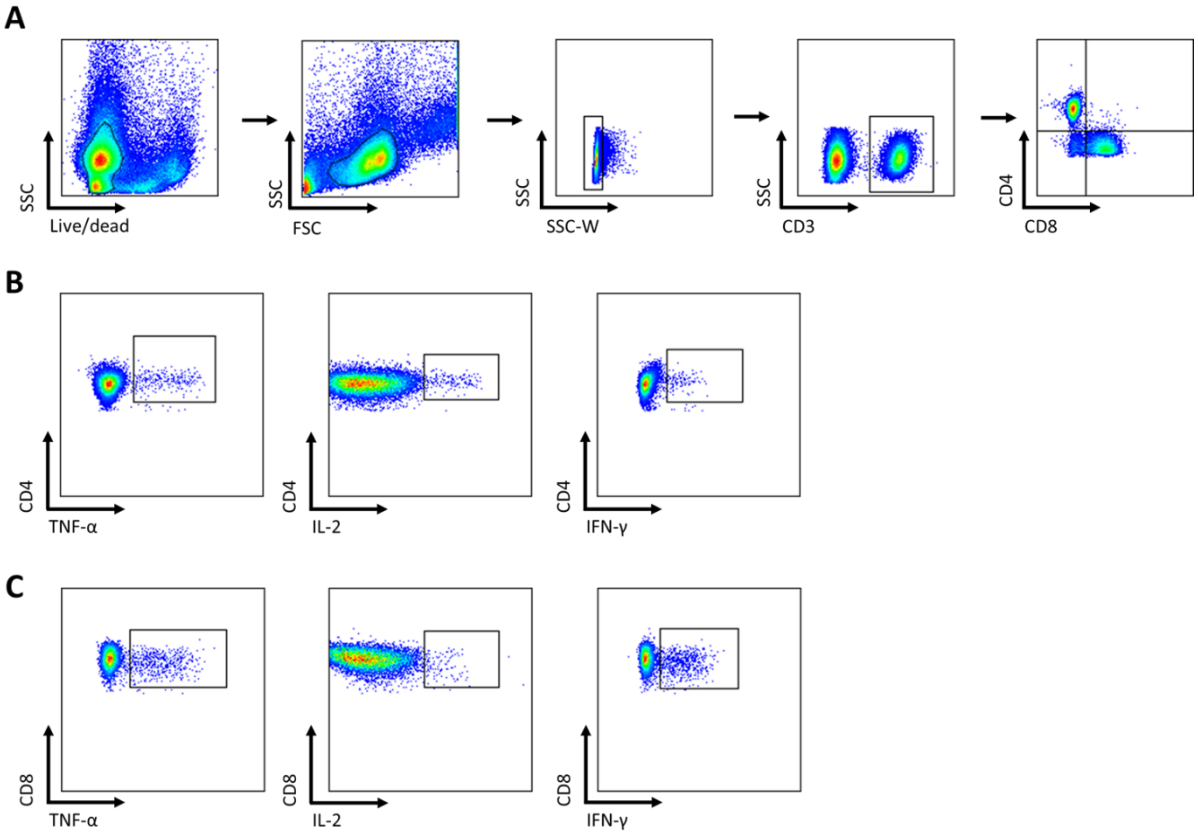

Figure S2. Representative gating strategy used for the analysis of T cell responses in spleens. **A)** Gating of live T cells ($CD3^+$). **B)** Cytokine-producing $CD4^+$ T cells. **C)** Cytokine-producing $CD8^+$ T cells.

Biodistribution of SAM-LNPs

The pharmacokinetics of adjuvants can influence the immune responses elicited to a subunit antigen [27, 28]. Therefore, we investigated the biodistribution of DOTAP-cLNPs, DDA-cLNPs and iLNPs in mice following intramuscular administration. All three formulations accumulated at the injection site (Fig. 5A). High radiance was detected at the injection site for up to 10 days, whilst no detectable signal was observed in other organs during the course of the experiments. However, DOTAP-cLNPs and iLNPs were cleared significantly ($p<0.05$) faster than DDA-cLNPs, as evidenced by the calculated areas under the curve (Fig. 5B), despite their similar general physico-chemical characteristics (Table 1).

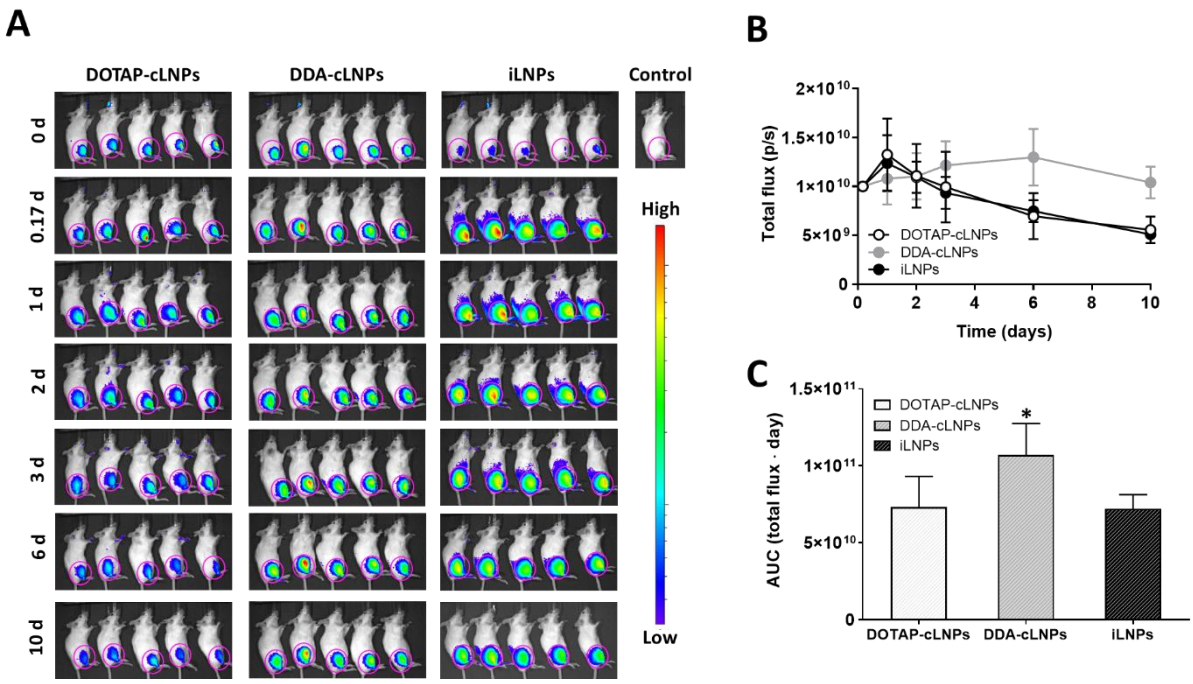

Figure 5. Biodistribution of DOTAP-cLNPs, DDA-cLNPs and benchmark iLNPs in mice following intramuscular administration. **A)** Images acquired at relevant time points. **B)** Biodistribution pharmacokinetics. **C)** Calculated areas under the curve for each formulation. Results are represented as total flux in the region of interest, in pink, as mean ± SD of five animals per group. Statistical significance of DDA-cLNPs compared to DOTAP-cLNPs and iLNPs: $p < 0.05$ (*).

Discussion

All cLNP and iLNP formulations were monodisperse, with a hydrodynamic diameter from 66 to 102 nm, neutral zeta-potential (<5 mV) and high SAM encapsulation efficiency (>85%), with the exception of DSTAP-cLNPs (size>300 nm; PDI>0.4; SAM E.E.<75%, Table 1). These findings are in agreement with recent investigations conducted by Patel and colleagues [17], where both particle size and mRNA E.E. highly depended on the type of cationic lipid. The improved in vitro potency (Fig. 2) of DOTAP and DDA-based cLNPs over DC-Chol, DMTAP and DOBAQ could be related to the ability of these lipids to pack and stabilize SAM. Similar conclusions were reported in studies conducted by Regelin et al. [29] with several DOTAP analogues being tested, including DOTAP, DMTAP and DSTAP among others. In their investigations, the higher transfection efficiency of DOTAP-containing lipoplexes was suggested to be directly related to the increased stability of these lipoplexes, as determined by anisotropy measurements. Despite DC-Chol-based lipoplexes have been widely described as efficient pDNA and siRNA transfection systems [30], our DC-Chol-cLNPs were inefficient to deliver SAM *in vitro* (Fig. 2). This lack of potency may be attributed to the DOPE:DC-Chol ratio used to formulate our cLNPs (1:1)

[31, 32]. Moreover, DOTAP and DDA-cLNPs were superior to benchmark iLNPs (Fig. 2). This was a likely consequence of the higher cellular association of DOTAP and DDA-cLNPs compared to iLNPs (Fig. 1). While the presence of constitutively charged lipids allows cLNPs to interact with cells [33, 34], benchmark iLNPs and require ApoE to be taken up by cells. Hence, iLNPs are unable to induce antigen expression in serum-free medium [35]. Therefore, DOTAP and DDA-cLNPs were chosen for further in vivo investigations. Nonetheless, in vitro transfection studies are a poor predictor of immunogenicity [16] and benchmark iLNPs were expected to outperform cLNPs in vivo, as previously reported elsewhere [13]. Notably, within our studies, only at the low dose (0.15 μg) and after a booster injection did iLNPs significantly outperform cLNPs; at a dose of 1.5 μg RVG-SAM after the first and second vaccination iLNPs and cLNPs IgG titers were not significantly different (Fig. 4). However, iLNPs were significantly ($p<0.05$) better at inducing $CD8^+$ (C) and $CD4^+$ T cell responses (Fig. 4).

Although a schedule of few administrations given weeks or months apart is preferred for the induction of protective immune responses, the induction of protective immunity after a single vaccination is highly desirable for prophylactic vaccines. Previous studies have demonstrated that LNP-formulated mRNA vaccines can induce quick and durable immune responses in mice and non-human primates [36, 37]. RVG-SAM nanosystems induced more rapid antibody responses than Rabipur after the first vaccination. The differences between RVG-SAM formulations and Rabipur were less evident after the boost dose. It is worth underlying that differences in potency among vaccines can be veiled by further booster vaccinations. The immunization strategy can influence the immunogenicity of a vaccine, and variations in intervals between immunizations may result in different levels and qualities of the immune response [38].

DOTAP and DDA have been widely used to deliver nucleic acid-based vaccines for infectious diseases and cancer immunotherapy [39-43] due to their unique ability to condense nucleic acids. When considering these formulations, there is the potential of self-adjuvanticity from both the RNA and the lipid system [44, 45]. Given that all formulations had the same SAM this would be negated in this study. With regard to comparing between the lipids, DDA has been previously shown to be more immunogenic than DOTAP [15]. However, within these studies we saw no significant difference between the DOTAP and the DDA formulations. Similar findings were reported by Blakney et al., in whose studies DOTAP and DDA-cLNPs induced equivalent antigen expression [41] and immune responses in vivo [46]. Although cationic and ionizable lipids could play a role in the immunostimulation of immune cells, their effect would likely be masked by the immunostimulatory properties of SAM. For instance, DOTAP-cLNPs and iLNPs only stimulated antigen-presenting cells in vivo when formulated with mRNA [42, 47].

Within our studies, we demonstrate that cLNPs and iLNPs formed depots at the injection site, with DDA-based systems remaining longer at the injection site. No detectable signal was observed in organs during the course of the experiment, as have previously shown with similar DDA formulations [22].The retention of liposomal DNA vaccines (composed of PC, DOPE and DOTAP) at the injection site has also been previously shown using radiolabelled trackers [48]. In vivo gene expression at the injection site after administration with LNPs containing SAM encoding luciferase has also been shown with high levels bioluminescence at day 3, which peaked at day 7, and decreased to background by day 63 [4]. The impact of cationic lipid on the formulation of a depot and the slower clearance of DDA based formulations from the injection site has also been noted with liposomal adjuvants; DDA:TDB liposomes and their associated antigen were retained significantly longer than DOTAP:TDB liposomes, and the higher depot effect created by DDA-based liposomes correlated with increased immunogenicity compared to the DOTAP formulation [15]. The addition of a PEGylated lipid (25 mole %) to these DDA based formulations was shown to block the depot effect and impact on the immunological activity of the liposomal adjuvants [49]. However, from the results in Fig. 4 and 5 there is no clear link between LNP retention at the injection site and immunological activity.

Upon administration of mRNA vaccines formulated in lipid particles, a range of immune cells are recruited at the injection site [7, 47]. It has been hypothesized that myocytes are the main cell type transfected upon intramuscular administration of mRNA vaccines, which act as a source of antigen for APCs to cross-prime T cells [50]. Based on this, immunization with LNP-formulated mRNA vaccines could increase numbers of effector cells at the local lymph nodes compared to naked mRNA [36] by facilitating its delivery to immune cells. However, a high accumulation of delivery system in the lymphatics does not necessarily translate into higher immunogenicity [51] and the influence of the depot effect on nucleic acid vaccines is not clear; for example, plasmid DNA (pDNA)-lipoplexes of 140 nm elicited stronger immune responses than 560 nm lipoplexes despite their more rapid clearance from the injection site [48]. In a recent investigation by Hassett et al., it was suggested that the accumulation of LNPs at the injection site may not be required for mRNA-LNPs to elicit robust immune responses. In their studies, 5 biodegradable iLNPs induced significantly higher production of antibodies compared to MC3-iLNPs notwithstanding their significantly faster clearance (<5% injected dose 24 hours post injection) compared to MC3-iLNPs (50% injected dose 24 hours post-injection) [13]. Furthermore,

within our biodistribution studies, our formulations were labelled with the fluorescent dye DiR, commonly used as a membrane marker. On degradation of LNPs, staining of muscle cells could result. However, preliminary studies using Förster resonance energy transfer (FRET) performed in our

research group with cationic liposomes suggest that this formulation is not degraded over a period of at least four days (unpublished results). Tracking biodistribution of LNPs using IVIS only allows a general tracking of particles and does not allow us to discriminate particles remaining in the extracellular matrix from those phagocyted or surface-adsorbed and a single cell assay, e.g. confocal microscopy, could be used to determine the cellular localization of the particles. Cell recruitment studies as those described in [7] and [36], as well as the analysis of relevant organs at earlier time points could therefore be conducted to add further insight into differences in formulations. Indeed work by Luz et al. [36] reported that the intramuscular injection of an LNP-formulated RVG-mRNA vaccine resulted in a local increase in TNF-α, IL-6, MIP-1β and CCXL9 concentrations at the injection site that was not observed in mice immunized with unformulated mRNA. This increased cell numbers at the local lymph nodes and a strong activation of activated innate and adaptive immune cells at the local lymph nodes. Brito et al. [7] showed that the administration of a SAM vaccine formulated in MF59 (a trademark of GSK group of companies) and DOTAP-CNE (an MF59 formulation containing DOTAP) resulted in the attraction of similar numbers of leukocytes to the injection site. However, MF59-formulated SAM was significantly less immunogenic than the DOTAP-CNE. Altogether, these findings demonstrate that mRNA vaccines formulated in lipid systems benefit from protection against degradation, efficient delivery and a broad a transient local immunostimulatory environment that is important for the induction of subsequent adaptive immune responses.

Conclusions

We have demonstrated that cationic lipid nanoparticles (cLNPs) based on conventional cationic lipids are delivery systems for self-amplifying RNA (SAM) vaccines. All SAM-cLNP formulations prepared by microfluidic mixing were below 100 nm, monodisperse, with neutral zeta-potential and high SAM encapsulation efficiency (with the exception of DSTAP-based formulations). All formulations interacted with cells in vitro, with cLNPs containing the fusogenic lipid DOPE and either DOTAP or DDA induced higher percentages of antigen expression than benchmark ionizable LNPs (iLNPs). These differences were more evident in absence of serum proteins. Although DOTAP and DDA-cLNPs were less immunogenic than iLNPs at lower concentrations and after 2 injections, they gave comparable IgG responses to iLNPs at 1.5 ug RVG-SAM after both a single and booster injection. cLNPs were also as potent as the commercial vaccine Rabipur and a DOTAP-based cationic nanoemulsion (DOTAP-CNE), and produced IgG titers above the protection threshold for protection against rabies infection and offer an alternative approach for as a safe and well-established SAM delivery vehicle.

Acknowledgements.

This work was funded by the European Commission Project *Leveraging Pharmaceutical Sciences and Structural Biology Training to Develop 21st Century Vaccines* (H2020-MSCA-ITN-2015 grant agreement 675370) and Independent Research Fund Denmark (7026-00027B) (S.S.). We thank the SAM Vaccine Platform Team at GSK Vaccines Rockville. We also thank the staff at the Animal Research Center and at the Flow-Cy-TOF Core Facility at GSK Vaccines Siena for technical assistance. The data that support the findings are openly available through the University of Strathclyde pureportal at [DOI to be confirmed on acceptance of paper].

Conflicts of interest

Gustavo Lou and Giulia Anderluzzi participated in the European Marie Curie PHA-ST-TRAIN-VAC PhD project at the University of Strathclyde (Glasgow, UK) in collaboration with GSK (Siena, Italy). This project was co-sponsored between the University of Strathclyde and GSK. Stuart Woods, Signe Tandrup Schmidt, Craig W. Roberts and Yvonne Perrie declare no conflict of interest. Simona Gallorini, Michela Brazzoli, Fabiola Giusti, Ilaria Ferlenghi, Russell Johnson, Derek T. O'Hagan and Barbara C. Baudner are employees of the GSK group of companies. All the authors declare that they have no other relevant affiliations or financial interest in conflict with the subject matter or materials discussed in the manuscript.

Author contribution

Gustavo Lou: Conceptualization, methodology, software, formal analysis, investigation, validation, resources, writing – original draft, writing – review and editing, visualization. **Giulia Anderluzzi:** Methodology, validation, resources, writing – review and editing. **Signe Tandrup Schmidt:** Methodology, validation, resources, writing – review and editing. **Stuart Woods:** Methodology, validation, resources, writing – review and editing. **Simona Gallorini:** Methodology, validation, resources, writing – review and editing, supervision. **Michela Brazzoli:** Conceptualization, methodology, validation, resources, writing – review and editing, supervision. **Fabiola Giusti:** Methodology, validation, resources, writing – review and editing. **Ilaria Ferlenghi:** Methodology, validation, resources, writing – review and editing. **Russell Johnson:** Conceptualization, methodology, validation, resources, writing – review and editing, supervision. **Craig W. Roberts:** Methodology, validation, resources, writing – review and editing, supervision. **Derek T. O'Hagan:** Conceptualization, methodology, validation, resources, writing – review and editing, supervision, funding acquisition and project management of PHA-ST-TRAIN-VAC. **Barbara C. Baudner:** Conceptualization, methodology,

validation, resources, writing – review and editing, supervision, funding acquisition and project management of PHA-ST-TRAIN-VAC. **Yvonne Perrie:** Conceptualization, methodology, validation, resources, writing – review and editing, visualization, supervision, funding acquisition and project management of PHA-ST-TRAIN-VAC

References

[1] J.A. Wolff, R.W. Malone, P. Williams, W. Chong, G. Acsadi, A. Jani, P.L. Felgner, Direct gene transfer into mouse muscle in vivo, Science, 247 (1990) 1465-1468.

[2] D.C. Tang, M. DeVit, S.A. Johnston, Genetic immunization is a simple method for eliciting an immune response, Nature, 356 (1992) 152-154.

[3] G. Maruggi, C. Zhang, J. Li, J.B. Ulmer, D. Yu, mRNA as a Transformative Technology for Vaccine Development to Control Infectious Diseases, Molecular Therapy, 27 (2019) 757-772.

[4] A.J. Geall, A. Verma, G.R. Otten, C.A. Shaw, A. Hekele, K. Banerjee, Y. Cu, C.W. Beard, L.A. Brito, T. Krucker, D.T. O'Hagan, M. Singh, P.W. Mason, N.M. Valiante, P.R. Dormitzer, S.W. Barnett, R. Rappuoli, J.B. Ulmer, C.W. Mandl, Nonviral delivery of self-amplifying RNA vaccines, Proc Natl Acad Sci U S A, 109 (2012) 14604-14609.

[5] A.B. Vogel, L. Lambert, E. Kinnear, D. Busse, S. Erbar, K.C. Reuter, L. Wicke, M. Perkovic, T. Beissert, H. Haas, S.T. Reece, U. Sahin, J.S. Tregoning, Self-Amplifying RNA Vaccines Give Equivalent Protection against Influenza to mRNA Vaccines but at Much Lower Doses, Molecular Therapy, 26 (2018) 446-455.

[6] J. Probst, S. Brechtel, B. Scheel, I. Hoerr, G. Jung, H.-G. Rammensee, S. Pascolo, Characterization of the ribonuclease activity on the skin surface, Genetic vaccines and therapy, 4 (2006) 4-4.

[7] L.A. Brito, M. Chan, C.A. Shaw, A. Hekele, T. Carsillo, M. Schaefer, J. Archer, A. Seubert, G.R. Otten, C.W. Beard, A.K. Dey, A. Lilja, N.M. Valiante, P.W. Mason, C.W. Mandl, S.W. Barnett, P.R. Dormitzer, J.B. Ulmer, M. Singh, D.T. O'Hagan, A.J. Geall, A Cationic Nanoemulsion for the Delivery of Next-generation RNA Vaccines, Molecular Therapy, 22 (2014) 2118-2129.

[8] T. Demoulins, P. Milona, P.C. Englezou, T. Ebensen, K. Schulze, R. Suter, C. Pichon, P. Midoux, C.A. Guzman, N. Ruggli, K.C. McCullough, Polyethylenimine-based polyplex delivery of self-replicating RNA vaccines, Nanomedicine, 12 (2016) 711-722.

[9] R. Goswami, D. Chatzikleanthous, G. Lou, F. Giusti, A. Bonci, M. Taccone, M. Brazzoli, S. Gallorini, I. Ferlenghi, F. Berti, D.T. O'Hagan, C. Pergola, B.C. Baudner, R. Adamo, Mannosylation of LNP Results in Improved Potency for Self-Amplifying RNA (SAM) Vaccines, ACS Infectious Diseases, (2019).

[10] M. Jayaraman, S.M. Ansell, B.L. Mui, Y.K. Tam, J. Chen, X. Du, D. Butler, L. Eltepu, S. Matsuda, J.K. Narayanannair, K.G. Rajeev, I.M. Hafez, A. Akinc, M.A. Maier, M.A. Tracy, P.R. Cullis, T.D. Madden, M. Manoharan, M.J. Hope, Maximizing the potency of siRNA lipid nanoparticles for hepatic gene silencing in vivo, Angew Chem Int Ed Engl, 51 (2012) 8529-8533.

[11] J.M. Richner, S. Himansu, K.A. Dowd, S.L. Butler, V. Salazar, J.M. Fox, J.G. Julander, W.W. Tang, S. Shresta, T.C. Pierson, G. Ciaramella, M.S. Diamond, Modified mRNA Vaccines Protect against Zika Virus Infection, Cell, 168 (2017) 1114-1125.e1110.

[12] A. Hekele, S. Bertholet, J. Archer, D.G. Gibson, G. Palladino, L.A. Brito, G.R. Otten, M. Brazzoli, S. Buccato, A. Bonci, D. Casini, D. Maione, Z.Q. Qi, J.E. Gill, N.C. Caiazza, J. Urano, B. Hubby, G.F. Gao, Y. Shu, E. De Gregorio, C.W. Mandl, P.W. Mason, E.C. Settembre, J.B. Ulmer, J. Craig Venter, P.R. Dormitzer, R. Rappuoli, A.J. Geall, Rapidly produced SAM(®) vaccine against H7N9 influenza is immunogenic in mice, Emerg Microbes Infect, 2 (2013) e52-.

[13] K.J. Hassett, K.E. Benenato, E. Jacquinet, A. Lee, A. Woods, O. Yuzhakov, S. Himansu, J. Deterling, B.M. Geilich, T. Ketova, C. Mihai, A. Lynn, I. McFadyen, M.J. Moore, J.J. Senn, M.G. Stanton, Ö. Almarsson, G. Ciaramella, L.A. Brito, Optimization of Lipid Nanoparticles for Intramuscular Administration of mRNA Vaccines, Molecular Therapy - Nucleic Acids, 15 (2019) 1-11.

[14] K.J. Kauffman, J.R. Dorkin, J.H. Yang, M.W. Heartlein, F. DeRosa, F.F. Mir, O.S. Fenton, D.G. Anderson, Optimization of Lipid Nanoparticle Formulations for mRNA Delivery in Vivo with Fractional Factorial and Definitive Screening Designs, Nano Letters, 15 (2015) 7300-7306.

[15] M. Henriksen-Lacey, D. Christensen, V.W. Bramwell, T. Lindenstrom, E.M. Agger, P. Andersen, Y. Perrie, Comparison of the depot effect and immunogenicity of liposomes based on dimethyldioctadecylammonium (DDA), 3beta-[N-(N',N'-Dimethylaminoethane)carbomyl] cholesterol (DC-Chol), and 1,2-Dioleoyl-3-trimethylammonium propane (DOTAP): prolonged liposome retention mediates stronger Th1 responses, Molecular pharmaceutics, 8 (2011) 153-161.

[16] S.E. McNeil, A. Vangala, V.W. Bramwell, P.J. Hanson, Y. Perrie, Lipoplexes formulation and optimisation: in vitro transfection studies reveal no correlation with in vivo vaccination studies, Curr Drug Deliv, 7 (2010) 175-187.
[17] S. Patel, R.C. Ryals, K.K. Weller, M.E. Pennesi, G. Sahay, Lipid nanoparticles for delivery of messenger RNA to the back of the eye, Journal of Controlled Release, 303 (2019) 91-100.
[18] H.C.J. Ertl, Novel vaccines to human rabies, PLoS neglected tropical diseases, 3 (2009) e515-e515.
[19] G. Lou, G. Anderluzzi, S. Woods, C.W. Roberts, Y. Perrie, A novel microfluidic-based approach to formulate size-tuneable large unilamellar cationic liposomes: Formulation, cellular uptake and biodistribution investigations, European Journal of Pharmaceutics and Biopharmaceutics, 143 (2019) 51-60.
[20] M. Feyssaguet, L. Dacheux, L. Audry, A. Compoint, J.L. Morize, I. Blanchard, H. Bourhy, Multicenter comparative study of a new ELISA, PLATELIA™ RABIES II, for the detection and titration of anti-rabies glycoprotein antibodies and comparison with the rapid fluorescent focus inhibition test (RFFIT) on human samples from vaccinated and non-vaccinated people, Vaccine, 25 (2007) 2244-2251.
[21] S. Gallorini, M. Taccone, A. Bonci, F. Nardelli, D. Casini, A. Bonificio, S. Kommareddy, S. Bertholet, D.T. O'Hagan, B.C. Baudner, Sublingual immunization with a subunit influenza vaccine elicits comparable systemic immune response as intramuscular immunization, but also induces local IgA and TH17 responses, Vaccine, 32 (2014) 2382-2388.
[22] D. Chatzikleanthous, S.T. Schmidt, G. Buffi, I. Paciello, R. Cunliffe, F. Carboni, M.R. Romano, D.T. O'Hagan, U. D'Oro, S. Woods, C.W. Roberts, Y. Perrie, R. Adamo, Design of a novel vaccine nanotechnology-based delivery system comprising CpGODN-protein conjugate anchored to liposomes, Journal of Controlled Release, (2020).
[23] P.R. Cullis, M.J. Hope, Lipid Nanoparticle Systems for Enabling Gene Therapies, Molecular Therapy, 25 (2017) 1467-1475.
[24] Z.Q. Xiang, B.B. Knowles, J.W. McCarrick, H.C.J. Ertl, Immune Effector Mechanisms Required for Protection to Rabies Virus, Virology, 214 (1995) 398-404.
[25] T.J. Wiktor, Cell-mediated immunity and postexposure protection from rabies by inactivated vaccines of tissue culture origin, Dev Biol Stand, 40 (1978) 255-264.
[26] M. Schnee, A.B. Vogel, D. Voss, B. Petsch, P. Baumhof, T. Kramps, L. Stitz, An mRNA Vaccine Encoding Rabies Virus Glycoprotein Induces Protection against Lethal Infection in Mice and Correlates of Protection in Adult and Newborn Pigs, PLoS neglected tropical diseases, 10 (2016) e0004746-e0004746.
[27] M. Henriksen-Lacey, V.W. Bramwell, D. Christensen, E.-M. Agger, P. Andersen, Y. Perrie, Liposomes based on dimethyldioctadecylammonium promote a depot effect and enhance immunogenicity of soluble antigen, Journal of Controlled Release, 142 (2010) 180-186.
[28] R. Kaur, V.W. Bramwell, D.J. Kirby, Y. Perrie, Manipulation of the surface pegylation in combination with reduced vesicle size of cationic liposomal adjuvants modifies their clearance kinetics from the injection site, and the rate and type of T cell response, Journal of controlled release : official journal of the Controlled Release Society, 164 (2012) 331-337.
[29] A.E. Regelin, S. Fankhaenel, L. Gürtesch, C. Prinz, G. von Kiedrowski, U. Massing, Biophysical and lipofection studies of DOTAP analogs, Biochimica et Biophysica Acta (BBA) - Biomembranes, 1464 (2000) 151-164.
[30] Y. Zhang, H. Li, J. Sun, J. Gao, W. Liu, B. Li, Y. Guo, J. Chen, DC-Chol/DOPE cationic liposomes: a comparative study of the influence factors on plasmid pDNA and siRNA gene delivery, Int J Pharm, 390 (2010) 198-207.
[31] M. Muñoz-Úbeda, A. Rodríguez-Pulido, A. Nogales, A. Martín-Molina, E. Aicart, E. Junquera, Effect of Lipid Composition on the Structure and Theoretical Phase Diagrams of DC-Chol/DOPE-DNA Lipoplexes, Biomacromolecules, 11 (2010) 3332-3340.

[32] Y. Maitani, S. Igarashi, M. Sato, Y. Hattori, Cationic liposome (DC-Chol/DOPE=1:2) and a modified ethanol injection method to prepare liposomes, increased gene expression, Int J Pharm, 342 (2007) 33-39.
[33] P. Harvie, F.M.P. Wong, M.B. Bally, Use of Poly(ethylene glycol)–Lipid Conjugates to Regulate the Surface Attributes and Transfection Activity of Lipid–DNA Particles, Journal of Pharmaceutical Sciences, 89 (2000) 652-663.
[34] S. Takano, Y. Aramaki, S. Tsuchiya, Physicochemical Properties of Liposomes Affecting Apoptosis Induced by Cationic Liposomes in Macrophages, Pharmaceutical Research, 20 (2003) 962-968.
[35] A. Akinc, W. Querbes, S. De, J. Qin, M. Frank-Kamenetsky, K.N. Jayaprakash, M. Jayaraman, K.G. Rajeev, W.L. Cantley, J.R. Dorkin, J.S. Butler, L. Qin, T. Racie, A. Sprague, E. Fava, A. Zeigerer, M.J. Hope, M. Zerial, D.W.Y. Sah, K. Fitzgerald, M.A. Tracy, M. Manoharan, V. Koteliansky, A.d. Fougerolles, M.A. Maier, Targeted delivery of RNAi therapeutics with endogenous and exogenous ligand-based mechanisms, Molecular therapy : the journal of the American Society of Gene Therapy, 18 (2010) 1357-1364.
[36] J. Lutz, S. Lazzaro, M. Habbeddine, K.E. Schmidt, P. Baumhof, B.L. Mui, Y.K. Tam, T.D. Madden, M.J. Hope, R. Heidenreich, M. Fotin-Mleczek, Unmodified mRNA in LNPs constitutes a competitive technology for prophylactic vaccines, npj Vaccines, 2 (2017) 29.
[37] N. Pardi, M.J. Hogan, R.S. Pelc, H. Muramatsu, H. Andersen, C.R. DeMaso, K.A. Dowd, L.L. Sutherland, R.M. Scearce, R. Parks, W. Wagner, A. Granados, J. Greenhouse, M. Walker, E. Willis, J.-S. Yu, C.E. McGee, G.D. Sempowski, B.L. Mui, Y.K. Tam, Y.-J. Huang, D. Vanlandingham, V.M. Holmes, H. Balachandran, S. Sahu, M. Lifton, S. Higgs, S.E. Hensley, T.D. Madden, M.J. Hope, K. Karikó, S. Santra, B.S. Graham, M.G. Lewis, T.C. Pierson, B.F. Haynes, D. Weissman, Zika virus protection by a single low-dose nucleoside-modified mRNA vaccination, Nature, 543 (2017) 248-251.
[38] L. Zhang, W. Wang, S. Wang, Effect of vaccine administration modality on immunogenicity and efficacy, Expert Rev Vaccines, 14 (2015) 1509-1523.
[39] M. Tian, Z. Zhou, S. Tan, X. Fan, L. Li, N. Ullah, Formulation in DDA-MPLA-TDB Liposome Enhances the Immunogenicity and Protective Efficacy of a DNA Vaccine against Mycobacterium tuberculosis Infection, Frontiers in immunology, 9 (2018) 310.
[40] M. Melo, E. Porter, Y. Zhang, M. Silva, N. Li, B. Dobosh, A. Liguori, P. Skog, E. Landais, S. Menis, D. Sok, D. Nemazee, W.R. Schief, R. Weiss, D.J. Irvine, Immunogenicity of RNA Replicons Encoding HIV Env Immunogens Designed for Self-Assembly into Nanoparticles, Molecular therapy : the journal of the American Society of Gene Therapy, 27 (2019) 2080-2090.
[41] A.K. Blakney, P.F. McKay, B. Ibarzo Yus, J.E. Hunter, E.A. Dex, R.J. Shattock, The Skin You Are In: Design-of-Experiments Optimization of Lipid Nanoparticle Self-Amplifying RNA Formulations in Human Skin Explants, ACS nano, 13 (2019) 5920-5930.
[42] C. Pollard, J. Rejman, W. De Haes, B. Verrier, E. Van Gulck, T. Naessens, S. De Smedt, P. Bogaert, J. Grooten, G. Vanham, S. De Koker, Type I IFN counteracts the induction of antigen-specific immune responses by lipid-based delivery of mRNA vaccines, Molecular therapy : the journal of the American Society of Gene Therapy, 21 (2013) 251-259.
[43] R. Verbeke, I. Lentacker, L. Wayteck, K. Breckpot, M. Van Bockstal, B. Descamps, C. Vanhove, S.C. De Smedt, H. Dewitte, Co-delivery of nucleoside-modified mRNA and TLR agonists for cancer immunotherapy: Restoring the immunogenicity of immunosilent mRNA, Journal of Controlled Release, 266 (2017) 287-300.
[44] C. Iavarone, D.T. O'hagan, D. Yu, N.F. Delahaye, J.B. Ulmer, Mechanism of action of mRNA-based vaccines, Expert Rev Vaccines, 16 (2017) 871-881.
[45] T. Pepini, A.M. Pulichino, T. Carsillo, A.L. Carlson, F. Sari-Sarraf, K. Ramsauer, J.C. Debasitis, G. Maruggi, G.R. Otten, A.J. Geall, D. Yu, J.B. Ulmer, C. Iavarone, Induction of an IFN-Mediated Antiviral Response by a Self-Amplifying RNA Vaccine: Implications for Vaccine Design, J Immunol, 198 (2017) 4012-4024.

[46] A.K. Blakney, P.F. McKay, B.I. Yus, Y. Aldon, R.J. Shattock, Inside out: optimization of lipid nanoparticle formulations for exterior complexation and in vivo delivery of saRNA, Gene Therapy, (2019).
[47] F. Liang, G. Lindgren, A. Lin, E.A. Thompson, S. Ols, J. Röhss, S. John, K. Hassett, O. Yuzhakov, K. Bahl, L.A. Brito, H. Salter, G. Ciaramella, K. Loré, Efficient Targeting and Activation of Antigen-Presenting Cells In Vivo after Modified mRNA Vaccine Administration in Rhesus Macaques, Molecular Therapy, 25 (2017) 2635-2647.
[48] M.G. Carstens, M.G.M. Camps, M. Henriksen-Lacey, K. Franken, T.H.M. Ottenhoff, Y. Perrie, J.A. Bouwstra, F. Ossendorp, W. Jiskoot, Effect of vesicle size on tissue localization and immunogenicity of liposomal DNA vaccines, Vaccine, 29 (2011) 4761-4770.
[49] R. Kaur, V.W. Bramwell, D.J. Kirby, Y. Perrie, Pegylation of DDA:TDB liposomal adjuvants reduces the vaccine depot effect and alters the Th1/Th2 immune responses, Journal of controlled release : official journal of the Controlled Release Society, 158 (2012) 72-77.
[50] S. Lazzaro, C. Giovani, S. Mangiavacchi, D. Magini, D. Maione, B. Baudner, A.J. Geall, E. De Gregorio, U. D'Oro, C. Buonsanti, CD8 T-cell priming upon mRNA vaccination is restricted to bone-marrow-derived antigen-presenting cells and may involve antigen transfer from myocytes, Immunology, 146 (2015) 312-326.
[51] C.B. Roces, S. Khadke, D. Christensen, Y. Perrie, Scale-independent microfluidic production of cationic liposomal adjuvants and development of enhanced lymphatic targeting strategies, Molecular pharmaceutics, (2019).